Proceedings of the 6th Nordic Signal Processing Symposium - NORSIG 2004
June 9 - 11, 2004
Espoo, Finland

Image Denoising by Combined Quincunx and Separable Wavelet-Domain Wiener Filtering

Miroslav Vrankic[1], *Karen Egiazarian*[2], *and Atanas Gotchev*[2]

[1]University of Zagreb
Faculty of EE & CS
CROATIA
E-mail: mvrankic@zesoi.fer.hr
URL: http://www.zesoi.fer.hr/~mvrankic

[2]Tampere University of Technology
Institute of Signal Processing
FINLAND
E-mail: [karen, agotchev]@cs.tut.fi
URL: http://www.cs.tut.fi/~[karen, agotchev]

ABSTRACT

In this paper, wavelet shrinkage techniques that make use of wavelets defined on quincunx grid are explored in comparison with techniques involving wavelets defined on separable grid. In order to better exploit the advantages of the nonseparable transform and to surpass certain disadvantages of quincunx wavelets, the empirical wavelet-domain Wiener filtering that combines separable and quincunx wavelets is additionally investigated.

1. INTRODUCTION

In the field of image denoising wavelet shrinkage techniques have been established as a very attractive and efficient tool, based on the good localization and approximation properties of the underlying transform. In wavelet domain, a small number of high-valued detail coefficients represent areas around sharp transitions (edges) while the bulk of small and close to zero detail coefficients represents the smooth image regions. Hence the simple yet efficient idea of wavelet shrinkage-based image denoising: the wavelet coefficients of the noisy image smaller than a given threshold are set to zero and the higher coefficients are either left unchanged (hard thresholding) or reduced with the value of the threshold (soft thresholding). Afterwards, the noise-free image estimate is obtained by inverse wavelet transform. Since the wavelet shrinkage theory was pioneered by Donono and Johnstone [1], [2] many researchers contributed by suggesting translation-invariant processing [3] or sophisticated thresholding schemes [4], [5], [6].

The majority of the research in this field is based on separable wavelet families rather than nonseparable ones. The former are defined on rectangular grids and utilize separable sampling schemes (see Fig. 1). They allow for a simple realization of the corresponding fast wavelet transform (FWT), i.e. it is realized by using 1-D filter banks computing 1-D FWT along rows followed by 1-D FWT along columns of the image [7].

However, the separable sampling scheme causes the transform to be biased in horizontal, vertical, and diagonal directions even if other directions dominate in the initial image. Therefore, some nonlinear, e.g. thresholding operations on the wavelet coefficients may generate annoying artifacts in the reconstructed image in horizontal or vertical directions for which the human visual system is most sensitive. In order to obtain different orientational properties one should use wavelets based on nonseparable, i.e. truly 2-D sampling schemes.

In this paper, we explore the quincunx sampling scheme, the simplest among nonseparable sampling schemes, for its applicability to image denoising. We have applied two techniques: simple wavelet shrinkage and wavelet-domain Wiener filtering. In section 2, comparison of separable wavelet shrinkage and quincunx wavelet shrinkage is given. In section 3, the previous denoising results are used as an estimate of the clean image needed for the empirical wavelet-domain Wiener filtering. Our experiments show that the combination of quincunx wavelet shrinkage (for obtaining the pilot estimate of the clean image) and separable wavelet-domain Wiener filtering gives perceptually better results compared to the purely separable approach.

2. WAVELET SHRINKAGE: QUINCUNX VERSUS SEPARABLE WAVELETS

Properties of a given wavelet decomposition are highly affected with the underlying sampling scheme, i.e. with the way the image samples are divided into a number of cosets (phases). The separable sampling scheme depicted in Fig. 1 leads to dividing an image into four phases. In a similar manner the critically sampled filter bank used to realize the corresponding FWT will have four channels leading to one set of approximation coefficients and three sets (subimages, subbands) of detail coefficients for each decomposition level. The three detail subbands correspond to horizontal, vertical and diagonal details in the original image.

In the quincunx sampling scheme (Fig. 1 right) an image is being divided in only two distinct cosets. In the figure, the first coset is represented by gray circles and the second coset is represented by white circles. Such a sampling scheme is a basis for a two-channel critically sampled wavelet filter bank which results in one image of approximation coefficients and one image of detail coeffi-

cients for each decomposition level. Observing the filtering process in a domain of an undecimated image, the quincunx filters are affecting only the samples on a quincunx grid.

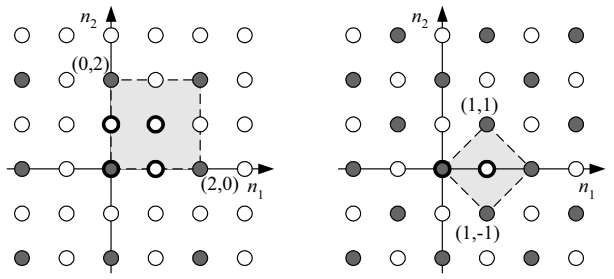

Fig. 1. Separable (left) and quincunx (right) sampling lattices. Samples belonging to the first phase for the given sampling scheme are marked with gray circles. The unit cell for each lattice is outlined with a dashed line and samples corresponding to it are bolded.

For the purpose of wavelet shrinkage, we have used quincunx interpolating filter banks designed by Kovacevic and Sweldens [8]. The filter bank has been designed by using the lifting scheme. In such a scheme (see Fig. 2), detail wavelet coefficients are obtained as an error of predicting samples (the *P* filter) from the second image phase based on a number of their surrounding samples from the first phase. The *U* filter is used to update the value of the average coefficients by using the already calculated detail coefficients. On the synthesis side, the reconstruction is easily performed by just inverting the order and signs of the predict and update steps [8]. We have used the simplest predict and update filters:

$$P(z_1,z_2) = 0.25\left(1+z_1^{-1}+z_2^{-1}+z_1^{-1}z_2^{-1}\right),$$
$$U(z_1,z_2) = 0.125\left(1+z_1+z_2+z_1z_2\right). \quad (1)$$

Therefore, one sample from the second quincunx phase is being calculated based on its four neighboring samples from the first quincunx phase. The resulting biorthogonal wavelet filter bank has 2 dual and 2 primal vanishing moments [8].

Since the decimated wavelet transform is not shift invariant, the denoising result will depend on the positions of the discontinuities in the image. Improved results can be obtained by using the undecimated version of the given wavelet transform [3]. In this paper, we will use the undecimated wavelet transforms only. In that case, the decimation operators are removed from the lifting scheme and the quincunx-upsampled versions of *P* and *U* filters are used.

For the separable wavelet transform thresholding is performed separately on the horizontal, vertical and diagonal detail coefficients. For the quincunx case, there is only one image of detail coefficients for every decomposition level. Since the quincunx upsampling of the filters causes their magnitude frequency responses to rotate for 45 degrees (see Fig. 3), every second decomposition level will have similar directional properties. It further means that in the first level (finest) detail coefficients the diagonal details will be much stronger than the horizontal and vertical ones, while in the second-stage detail coefficients (coarser ones) it will be opposite. In the third stage the relationships will be similar as in the first stage and so on. Such a property can be considered a drawback of the quincunx based wavelet transform because it is not easily possible to treat all the directions in the image similarly for all scales. On the other hand, in general, quincunx wavelets have the advantage versus the separable ones that the changes in the low-pass band between the two scales are more gradual. Therefore, to obtain similar level of smoothness of the denoised image one can typically use twice as many wavelet decomposition levels as in the separable case.

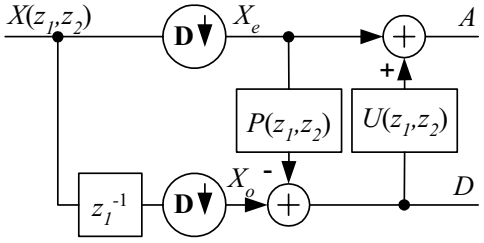

Fig. 2. Analysis quincunx filter bank based on the lifting scheme. The operator D↓ represents the quincunx downsampling.

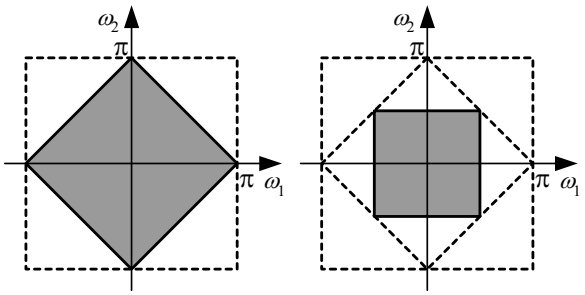

Fig. 3. Frequency supports of the idealized quincunx low-pass filter (left) and its quincunx-upsampled version (right).

In order to exploit quincunx wavelets in a better way, we have assigned different weights to all levels of the wavelet detail coefficients. In this way, for each decomposition level, the universal threshold has been multiplied with a different weight. The weights have been obtained empirically for a given quincunx wavelet family based on the measurement of the deviation of the detail coefficients of the image containing white Gaussian noise only. For levels from 1 to 8 (finest to coarsest) these weights are:
W = {2.5 1.5 0.9 0.8 0.7 0.6 0.5 0.4}.

In our experiments, we have used eight-level wavelet decomposition in the quincunx case as opposed to the four levels in the separable case.

3. WAVELET-DOMAIN WIENER FILTERING

In order to further improve the image denoising performance for the case of white Gaussian noise, a Wiener-like thresholding in wavelet domain has been suggested [4]. The optimal estimate of the original (noise-free) wavelet coefficients θ regarding the mean squared error (MSE) is obtained as

$$\hat{\theta}(i,j) = \underbrace{\frac{\theta^2(i,j)}{\theta^2(i,j)+\sigma^2}}_{H_W(i,j)} w(i,j)\,, \qquad (2)$$

where w denotes the wavelet coefficients of the noisy image $y = x + n$ (n stands for the white Gaussian noise), and σ is the noise deviation. In this way, each noisy wavelet coefficient is treated separately with a corresponding weight. In order to obtain the optimal Wiener filter it is necessary to know the wavelet coefficients of the original image x and the noise variance. The latter can be reliably estimated by using the median absolute deviation (MAD) of the wavelet coefficients on the finest level [9]. In order to circumvent the problem with the unknown original image, a two-stage procedure has been suggested in [4]. First, a pilot image estimate is obtained by preliminary wavelet shrinkage in a primary wavelet transform (see Fig. 4). Then, both noisy and pilot images are transformed to a secondary wavelet domain, where the empirical Wiener filter is applied:

$$\hat{\theta}_2(i,j) = \underbrace{\frac{\hat{\theta}_{21}^2(i,j)}{\hat{\theta}_{21}^2(i,j)+\hat{\sigma}^2}}_{\hat{H}_W(i,j)} w_2(i,j)\,. \qquad (3)$$

In this scenario the second transform is used to spread the primary wavelet-domain thresholded coefficients and to reevaluate them by weighting the noisy wavelet coefficients. The mismatch between the two wavelet transforms is exploited to obtain a more reliable estimate of the clean image [4].

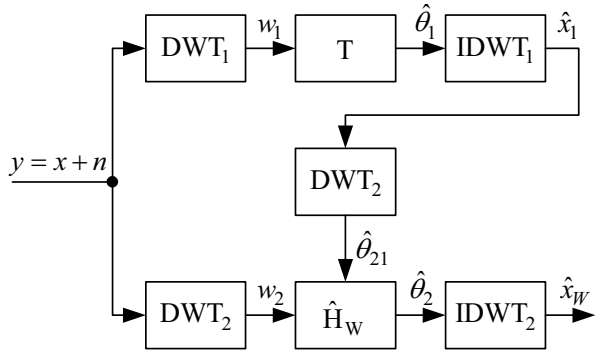

Fig. 4. Wavelet domain empirical Wiener filtering.

Our idea was to emphasize the mismatch by using the quincunx wavelets for the first stage and separable wavelets for the second stage.

4. RESULTS AND CONCLUSIONS

We have compared empirical Wiener filtering that uses quincunx wavelets in the primary transform and separable wavelets in the secondary one (denoted hereafter as Q+S scheme) with Wiener filtering that uses separable wavelets in both transforms (denoted as S+S scheme). For separable wavelet decomposition four decomposition levels have been used as opposed to eight levels for the wavelet decomposition defined on the quincunx grid. The Daubechies wavelets of order two (*db2*) have been used in the first stage, and symlet wavelets of order six (*sym6*) have been used in the second stage of the Wiener S+S scheme.

In Fig. 5, the denoising results are presented in terms of Peak Signal to Noise Ratio (PSNR) and Mean Absolute Error (MAE) between the clean and the denoised image. These results clearly show that the Wiener Q+S scheme performs better than the Wiener S+S scheme. It is also visible that the improvement in the final denoised image over the pilot estimate is lower when using the S+S scheme than when using the Q+S scheme. Such behavior is grounded by the fact that the wavelets used in the two stages of the Q+S scheme are mismatched more than the two families of separable wavelets used in the S+S scheme. Specifically, the preliminary thresholding in quincunx domain applies smaller relative threshold and introduces less Gibbs-like artifacts being also displaced from horizontal and vertical directions. They can be well eliminated by the secondary separable wavelet-domain Wiener filtering while preserving at the same time fine image details. Fig. 6 demonstrates the superiority of the Q+S scheme in terms of visual better preservation of small details. Additional improvement could be achieved by an adaptive quincunx wavelet filter banks based on the lifting scheme that is the topic of an outgoing research.

REFERENCES

[1] D. Donoho and I. Johnstone, "Ideal Spatial Adaptation via Wavelet Shrinkage", *Biometrica*, vol. 81, pp. 425-455, 1994.

[2] D. Donogo and I. Johnstone, "Adapting to Unknown Smoothness via Wavelet Shrinkage", *J. Amer. Stat. Assoc.*, vol. 90, pp. 1200-1224, 1995.

[3] R. Coifman and D. Donoho, "Translation-invariant Denoising", *in Wavelets and Statistics*, A. Antoniadis and G. Oppenheim (eds.), Springer-Verlag, pp. 125-150, 1995.

[4] Ghael and Baraniuk, "Improved Wavelet Denoising via Empirical Wiener Filtering", SPIE, 1995.

[5] M. Crouse, R. Novak, and R. Baraniuk, "Wavelet-based Statistical Signal Processing using Hidden Markov Models", IEEE Trans. Signal Processing, vol. 46, pp. 886-902, 1998.

[6] S. Grace Chang, B. Yu, and M. Vetterli, "Spatially Adaptive Wavelet Thresholding with Context Modeling for Image Denoising", IEEE Trans. Image Processing, vol. 9, pp. 1522-1531, 2000.

[7] S. G. Mallat, "A Theory for Multiresolution Signal Decomposition: The Wavelet Representation," *IEEE Trans. on Pattern Analysis and Machine Intelligence*, vol. 11, no. 7, pp. 647-693, July. 1989.

[8] J. Kovačević and W. Sweldens, "Wavelet Families of Increasing Order in Arbitrary Dimensions", *IEEE Trans. on Image Proc*, vol. 9, no. 3, pp. 480-496, March 2000.

[9] I. Johnstone and B. Silverman, "Wavelet Threshold Estimators for Data with Correlated Noise", *J. Royal Stat. Soc*., vol. B 59, pp. 319-351, 1997.

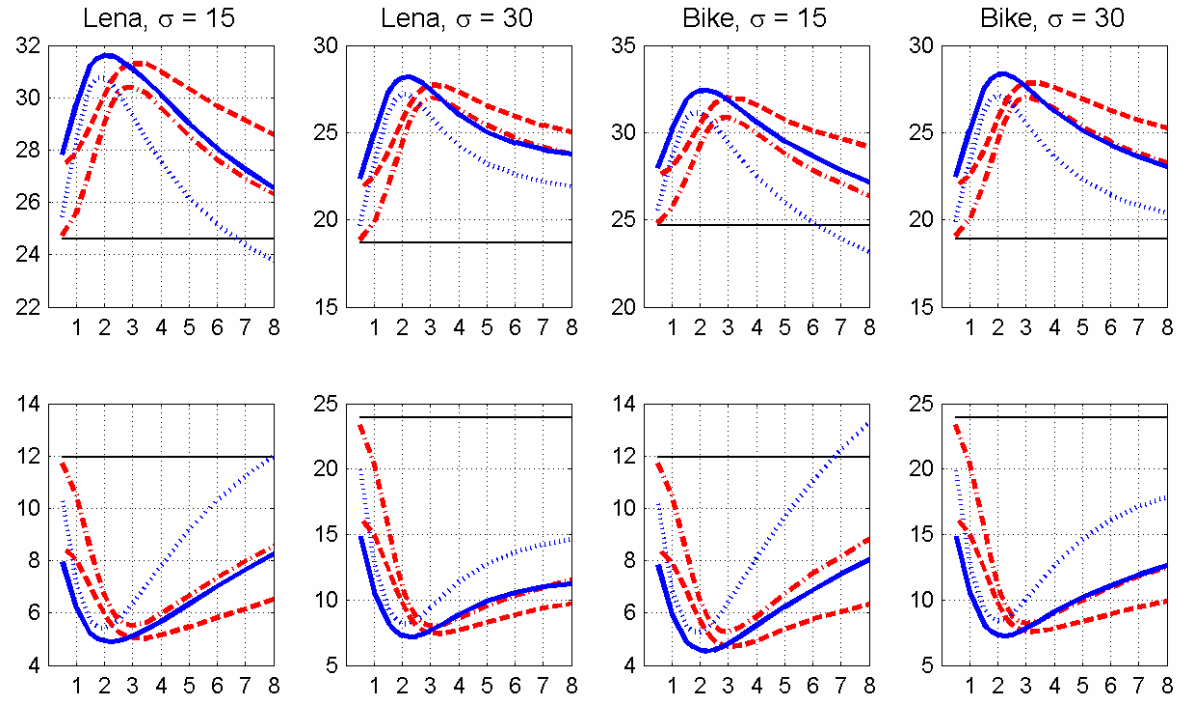

Fig. 5. PSNR (first row) and MAE (second row) of denoised images against the normalized threshold N. The results are given for central parts 200x200 pixels big of images Lena and Bike with added Gaussian noise with σ = 15 and 30. Dotted line: pilot estimate obtained by hard thresholding quincunx wavelet coefficients. Threshold $T_Q = N*\sigma*W$ (see text for W). Solid line: Q+S Wiener scheme. Dash-dot line: Pilot estimate obtained by separable wavelet hard thresholding. Threshold $T_S = N*\sigma$. Dashed line: S+S Wiener scheme. Horizontal solid line: Noisy image

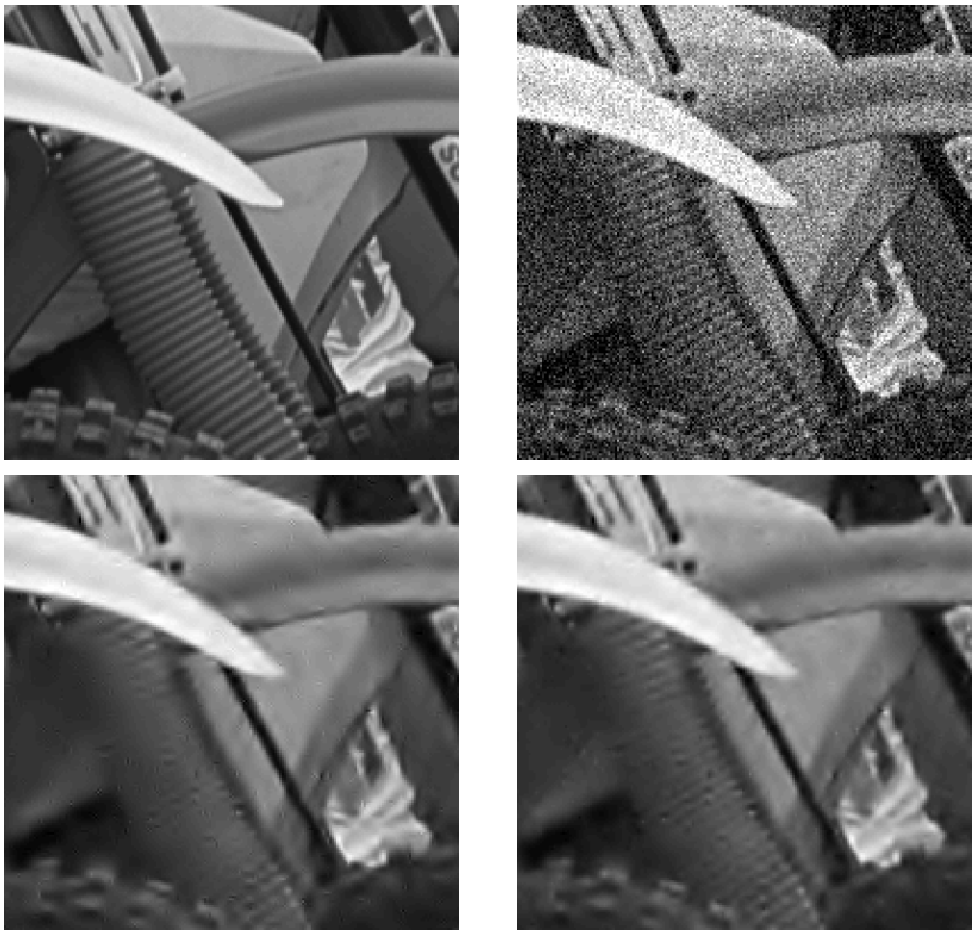

Fig. 6. Denoising the image Bike.
Left most: The central part 200x200 pixels big of the original Bike image.
Left: Gaussian noise with σ = 30 added to the original image.
Bottom left most: Wiener S+S scheme with pilot estimate obtained by soft thresholding. The threshold has been set to T_S =60.
Bottom left: Wiener Q+S scheme with pilot estimate obtained by soft thresholding the quincunx wavelet coefficients. The threshold has been set to T_Q = 45*W (see text for W). Note that the latter approach gives perceptually better results.